Diagnostic Value, Oncologic Outcomes, and Safety Profile of Image-Guided Surgery Technologies During Robot-Assisted Lymph Node Dissection with Sentinel Node Biopsy for Prostate Cancer

Elio Mazzone*[1], Paolo Dell'Oglio*[2,3,5], Nikos Grivas[3], Esther Wit[3], Maarten Donswijk[4], Alberto Briganti[1], Fijs Van Leeuwen[3,5], and Henk van der Poel[3]

[1]Department of Urology and Division of Experimental Oncology, Urological Research Institute, IRCCS San Raffaele Scientific Institute, Milan, Italy; [2]Department of Urology, ASST Grande Ospedale Metropolitano Niguarda, Milan, Italy; [3]Department of Urology, Antoni van Leeuwenhoek Hospital, The Netherlands Cancer Institute, Amsterdam, The Netherlands; [4]Department of Nuclear Medicine, Antoni van Leeuwenhoek Hospital, The Netherlands Cancer Institute, Amsterdam, The Netherlands; and [5]Interventional Molecular Imaging laboratory, Department of Radiology, Leiden University Medical Centre, Leiden, The Netherlands

Despite good sensitivity and a good negative predictive value, the implementation of sentinel node biopsy (SNB) in robot-assisted radical prostatectomy with extended pelvic lymph node dissection (ePLND) for prostate cancer is still controversial. For this reason, we aimed to define the added value of SNB (with different tracer modalities) to ePLND in the identification of nodal metastases. Complication rates and oncologic outcomes were also assessed. **Methods:** From January 2006 to December 2019, prospectively collected data were retrospectively analyzed from a single-institution database regarding prostate cancer patients treated with robot-assisted radical prostatectomy and ePLND with or without additional use of SNB, either with the hybrid tracer indocyanine green (ICG)–^{99m}Tc-nanocolloid or with free ICG. Multivariable logistic and Cox regression models tested the impact of adding SNB (either with the hybrid tracer or with free ICG) on lymph nodal invasion detection, complications, and oncologic outcomes. **Results:** Overall, 1,680 patients were included in the final analysis: 1,168 (69.5%) in the non-SNB group, 161 (9.6%) in the ICG-SNB group, and 351 (20.9%) in the hybrid-SNB group. The hybrid-SNB group (odds ratio, 1.61; 95%CI, 1.18–2.20; $P = 0.002$) was an independent predictor of nodal involvement, whereas the ICG-SNB group did not reach independent predictor status when compared with the non-SNB group (odds ratio, 1.35; 95%CI, 0.89–2.03; $P = 0.1$). SNB techniques were not associated with higher rates of complications. Lastly, use of hybrid SNB was associated with lower rates of biochemical recurrence (0.79; 95%CI, 0.63–0.98) and of clinical recurrence (hazard ratio, 0.76, $P = 0.035$) than were seen in the non-SNB group. **Conclusion:** The implementation of hybrid-SNB technique with ICG–^{99m}Tc-nanocolloid in prostate cancer improves detection of positive nodes and potentially lowers recurrence rates with subsequent optimization of patient management, without harming patient safety.

Key Words: image-guided surgery; indocyanine green; fluorescence; lymph node dissection; sentinel node biopsy; prostate cancer

During the last decade, there has been increasing interest in identifying and implementing new staging modalities for lymphatic metastatic dissemination in prostate cancer patients. An extended pelvic lymph node dissection (ePLND) represents the best available staging tool for prostate cancer patients with a risk of lymph node invasion (LNI) higher than 5% (*1*, *2*). Although this approach is invasive, it can still miss aberrant dissemination pathways to approximately 30% of lymph nodes—those that are outside the ePLND template (*2*). Tailored staging modalities that help predict the routes of lymphatic spread, such as sentinel node biopsy (SNB), have been proposed to improve the accuracy of ePLND in identifying nodal metastases (*3*, *4*). Despite the good sensitivity and good negative predictive value of SNB (*2*), its added value relative to ePLND in detecting LNI remains a subject of discussion. As a consequence, SNB in prostate cancer is still considered experimental (*2*). One concern is that the safety profile of adding SNB to ePLND, in terms of complications, has never been tested. Finally, evidence supporting the oncologic benefit of SNB and ePLND in prostate cancer is still limited and often controversial (*1*, *5–7*).

On this basis and to overcome these limitations, we used the largest available case series of patients who underwent robot-assisted radical prostatectomy and ePLND with or without SNB to define the effect of SNB and different SNB tracer modalities on LNI staging accuracy, complication rates, and midterm oncologic outcomes.

MATERIALS AND METHODS

Data Source and Patient Selection

From January 2006 to December 2019, prospectively collected data were retrospectively analyzed from a single-institution database (Antoni van Leeuwenhoek Hospital, The Netherlands Cancer Institute, Amsterdam) regarding prostate cancer patients treated with robot-assisted radical prostatectomy and standard ePLND with or without additional use of SNB. SNB was performed using either the hybrid fluorescent and radioactive tracer indocyanine green (ICG)–^{99m}Tc-nanocolloid or free ICG (*8–10*). We focused on patients with more than a 5% risk of LNI according to the nomogram of Briganti et al. (*11*), which has been found to be one of the most accurate predictive

models for LNI in external validation studies (*12*), particularly for the time span of our analysis. All surgeries were performed by the robotic approach, and all patients with complete follow-up pathologic data and recurrence data were included. Overall, 1,680 patients were included in the final analysis: 1,168 (69.5%) who were offered ePLND only (non-SNB group), 161 (9.6%) who received ePLND complemented by SNB using free ICG (ICG-SNB group), and 351 (20.9%) who received ePLND complemented by SNB using ICG–^{99m}Tc-nanocolloid (hybrid-SNB group). Patients receiving ePLND without SNB were treated between 2006 and 2019, those receiving ePLND and hybrid tracer were treated between 2010 and 2019, and those receiving ICG SNB were treated between 2016 and 2019.

The study protocol was approved by the institutions' medical ethics committees (approvals NL28143.031.09, NL41285.031.12, and NL46580.031.13). An approval from the institutional review board was received for the data collection and analysis.

SNB and ePLND Technique

The ePLND, SNB technique, and pathologic examination were previously described (*13*). Patients first underwent SNB, followed by ePLND and robot-assisted radical prostatectomy. Sentinel nodes (SNs) were identified via lymphatic mapping with ICG–^{99m}Tc-nanocolloid (0.5 mg of albumin, 0.25 mg of ICG, and 240 MBq of ^{99m}Tc in 2 mL of saline) or free ICG (5 mg in 2 mL of sterile water).

On the morning of the surgery, ICG–^{99m}Tc-nanocolloid (2 mL) was transrectally injected under ultrasound guidance into the peripheral zone of each quadrant of the prostate, as previously described (*14*, *15*). Early and late dynamic lymphoscintigraphy was performed at, respectively, 15 min and 2 h after injection. In the hybrid-SNB group, preoperative SN mapping was performed with lymphoscintigraphy and SPECT supplemented with low-dose CT (SPECT/CT). The nuclear medicine physician assessed all acquired images and reported the anatomic localization of the individual SNs. Surgery was planned to start 4 h after the ICG–^{99m}Tc-nanocolloid injection. All SNs were pursued with radioguidance and fluorescence guidance. The radioguidance was provided by the Europrobe laparoscopic 0° γ-probe (Eurorad S.A.) used in combination with a sterile cover. The fluorescence guidance was provided by the integrated FireFly camera of the DaVinci Si robotic system (Intuitive Surgical).

In the ICG-SNB group, 2 mL of ICG were transrectally injected in the operating room under ultrasound guidance before the surgery began. All SNs were pursued with FireFly fluorescence guidance (*15*) followed by an ePLND template, which was defined as the region encompassed by the ureteric crossing and including the bifurcation of the common iliac artery, along the external iliac (the distal limit being the deep circumflex vein and femoral canal), the internal iliac vessels, and the obturator fossa. The lateral border was the genitofemoral nerve, and the medial border was the perivesical fat. Thirteen surgeons were included in the current large cohort of individuals who performed robot-assisted radical prostatectomy, but the SNB procedures were performed exclusively by 3 surgeons.

Outcomes

The primary endpoint of our study was to assess the added value of SNB to ePLND in the identification of nodal metastases. Additionally, we tested the lymph node detection rate according to the preoperative LNI risk, based on the 2012 version of the nomogram of Briganti et al. (*11*). Secondary endpoints were the safety profile of SNB by reporting rates of postoperative complications and midterm oncologic outcomes, namely biochemical recurrence (BCR) and clinical recurrence (CR). BCR was defined as 2 consecutive prostate-specific antigen measures of at least 0.2 ng/mL (*2*). CR consisted of any radiologically confirmed locoregional or distant tumor recurrence. Postoperative complications were graded according to the Clavien–Dindo classification (*16*).

Variable Definition

The clinical covariates were age at surgery, use of neoadjuvant androgen deprivation therapy, clinical T stage (T1c, T2, T3), clinical N stage (Nx, N0, N1), biopsy Gleason score, and preoperative initial level of prostate-specific antigen. Pathologic and postoperative covariates consisted of pathologic T stage ($\leq$pT2, pT3a, $\geq$pT3b), pathologic N stage (pN0, pN1), pathologic Gleason score (*6–10*), number of lymph nodes removed, presence of positive surgical margins, and use of salvage radiation therapy.

Statistical Analysis

Statistical analyses, as well as reporting and interpretation of the results, were conducted according to established guidelines (*17*) and consisted of 4 steps. First, medians and interquartile ranges were reported for continuous variables, and frequencies and proportions were reported for categoric variables. The Mann–Whitney and χ^2 tests were applied to compare the statistical significance of differences in the distribution of continuous or categoric variables, respectively.

Second, multivariable logistic regression models were fitted to assess the impact of SNB (non-SNB group vs. hybrid-SNB group vs. ICG-SNB group) on LNI rate at the final pathologic examination, after adjusting for several clinical confounders. Models were adjusted using prespecified clinical covariates. Thereafter, the multivariable-derived probability of LNI detection according to different SNB methods was plotted against preoperative score according to the nomogram of Briganti et al. (*11*) using a locally weighted scatterplot smoother function (*18*, *19*), after accounting for the confounders.

Third, 2 sets of logistic regression models were fitted to test the impact of SNB use and type on postoperative complications, after adjusting for age at surgery, neoadjuvant androgen deprivation therapy, cT stage, cN stage, preoperative prostate-specific antigen level, and biopsy Gleason score. Logistic regression models were repeated for a Clavien–Dindo grade of at least II and at least III. Additionally, to test the hypothesis that refinements in SN technique may have impacted the complication rate, an interaction term between type of SN (non-SNB group vs. hybrid-SNB group vs. ICG-SNB group) and year of surgery was used.

Fourth, Kaplan–Meier plots were used to depict BCR- and CR-free survival after stratification according to non-SNB group versus hybrid-SNB group versus ICG-SNB group. Finally, multivariable Cox regression models tested for predictors of BCR and CR. Previously defined pathologic covariates were included as predictors in Cox regression models. Moreover, models predicting CR were further adjusted for the use of salvage radiation therapy. Analyses were performed using R software, version 3.6.3, and all tests were 2-sided with the significance level set at a P value of less than 0.05.

RESULTS

Patient Characteristics

Table 1 and Figure 1 depict the clinical characteristics of our cohort. Compared with the non-SNB group, the patients of the ICG-SNB group were older (67 vs. 65 y old, $P < 0.001$), and more had a Gleason score of 8–10 at biopsy (41.6% vs. 29.4%, $P < 0.001$) or cN1 at preoperative imaging (15.5% vs. 5.7%, < 0.001). No statistically significant differences in cT stage or prostate-specific antigen at surgery were recorded between the ICG-SNB and non-SNB groups. On the other hand, more of the patients in the hybrid-SNB group than in the non-SNB group had a Gleason score of 7 at biopsy (65.2% vs. 54%, $P < 0.001$), and fewer had cN1 at preoperative imaging (0.9% vs. 5.7%, < 0.001). When compared with the ICG-SNB group, fewer of the patients in the hybrid-SNB group had cN1 at preoperative imaging (0.9% vs. 15.5%, $P < 0.001$), and the hybrid-SNB group had a lower

TABLE 1
Patient Characteristics

Characteristic	Parameter	Overall	Non-SNB, n = 1,168 (69.5%)	ICG SNB, n = 161 (9.6%)	P, non-SNB vs. ICG SNB	Hybrid SNB, n = 351 (20.9%)	P, non-SNB vs. hybrid SNB	P, ICG SNB vs. hybrid SNB
PSA before treatment (ng/mL)	Median	9.5	9.7	9.4	0.6	9	0.002	0.1
	IQR	6.8–16	6.9–16	6.7–18		6.4–14		
Age (y)	Median	65	65	67	<0.001	65	0.1	<0.001
	IQR	60–69	60–68	64–71		60.5–69		
Briganti LNI risk*	Median	12.6	11.9	20.5	<0.001	12.4	0.4	<0.001
	IQR	6.1–30.5	5.6–29.1	10.9–41.7		6.2–29.2		
Biopsy GS	6	212 (12.6)	187 (16)	7 (4.3)	<0.001	18 (5.1)	<0.001	0.03
	7	954 (56.8)	638 (54.6)	87 (54)		229 (65.2)		
	8–10	514 (30.6)	343 (29.4)	67 (41.6)		104 (29.6)		
cT	cT1c	250 (14.9)	180 (15.4)	18 (11.2)	0.3	52 (14.8)	0.8	0.5
	cT2	941 (56)	655 (56.1)	94 (58.4)		192 (54.7)		
	≥cT3	489 (29.1)	333 (28.5)	49 (30.4)		107 (30.5)		
Percentage of positive cores	<33%	454 (27)	319 (27.3)	23 (14.3)	<0.001	112 (31.9)	0.2	<0.001
	33%–66%	711 (42.3)	504 (43.2)	67 (41.6)		140 (39.9)		
	>66%	515 (30.7)	345 (29.5)	71 (44.1)		99 (28.2)		
cN	cNx	387 (23)	323 (27.7)	3 (1.9)	<0.001	61 (17.4)	<0.001	<0.001
	cN0	1198 (71.3)	778 (66.6)	133 (82.6)		287 (81.8)		
	cN1	95 (5.7)	67 (5.7)	25 (15.5)		3 (0.9)		
Follow-up (mo)	Median	38	46.5	15	<0.001	35	<0.001	<0.001
	IQR	14–66	17–70	7–25		14–58		
Operative time (min)	Median	119	115	111	0.01	121	<0.001	<0.001
	IQR	100–126	99–128	97–121		113.5–131		
LNs removed	Median	12	11	20	<0.001	17	<0.001	<0.001
	IQR	8–18	6–15	17–25		11–21		
pN stage	pN0	1 302 (77.5)	947 (81.1)	103 (64)	<0.001	252 (71.8)	<0.001	<0.001
	pN1	378 (22.5)	221 (18.9)	58 (36)		99 (28.2)		
Pathologic GS	6	158 (9.4)	129 (11)	3 (1.9)	<0.001	26 (7.4)	0.1	<0.001
	7	1 116 (66.4)	754 (64.6)	131 (81.4)		231 (65.8)		
	8–10	406 (24.2)	285 (24.4)	27 (16.8)		94 (26.8)		
pT stage	≤pT2c	851 (50.7)	593 (50.8)	55 (34.2)	<0.001	203 (57.8)	0.005	<0.001
	pT3a	411 (24.5)	260 (22.3)	68 (42.2)		83 (23.6)		
	≥pT3b	418 (24.9)	315 (27)	38 (23.6)		65 (18.5)		
Positive nodes	>2	121 (7.2)	68 (5.8)	19 (11.8)	<0.001	34 (9.7)	<0.001	0.1
	0	1 302 (77.5)	948 (81.2)	102 (63.4)		252 (71.8)		
	1–2	257 (15.3)	152 (13)	40 (24.8)		65 (18.5)		
Surgical margins	Negative	1 054 (62.7)	712 (61)	102 (63.4)	0.6	240 (68.4)	0.01	0.3
	Positive	626 (37.3)	456 (39)	59 (36.6)		111 (31.6)		
Salvage radiotherapy	No	1 232 (73.3)	843 (72.2)	133 (82.6)	0.006	256 (72.9)	0.8	0.02
	Yes	448 (26.7)	325 (27.8)	28 (17.4)		95 (27.1)		

*According to nomogram of Briganti et al. (11).

PSA = prostate-specific antigen; IQR = interquartile range; GS = Gleason score; LN = lymph nodes.

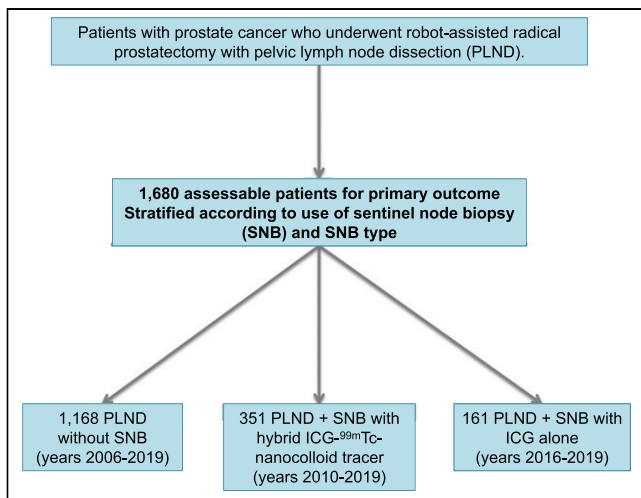Qualitative data are number followed by percentage in parentheses.

FIGURE 1. Flowchart describing final patient population included in study and implementation of different tracers for SNB over time.

median preoperative LNI risk score (12.4 vs. 20.5, $P < 0.001$). Regarding operative time, the ICG-SNB group had a shorter surgical median duration (111 min) than either the hybrid-SNB group (121 min) or the non-SNB group (115 min) ($P = 0.001$ and 0.01, respectively). Lastly, the rate of administration of salvage radiation therapy did not differ between the hybrid-SNB group (27.1%) and the non-SNB group (27.8%) ($P = 0.8$), whereas it was lower in ICG-SNB group (17.4%) than in either the hybrid-SNB group ($P = 0.02$) or the non-SNB group ($P = 0.006$).

Pathologic Report and Nodal Staging

Pathologic findings are reported in Table 1. Overall, in patients from the ICG-SNB group, disease was less frequently organ-confined ($\leq$pT2c: 34% vs. 50.8%, $P < 0.001$) than in the non-SNB group, and fewer had a Gleason score of 8–10 (16.8% vs. 24.4%, $P < 0.001$). Notably, the rate of pN1 in the ICG-SNB group was double that in the non-SNB group (36% vs. 18.9%, $P < 0.001$). Along the same line, the nodal yield increased for the ICG-SNB group (median, 20 vs. 11; $P < 0.001$), yielding a higher rate of patients with more than 2 positive nodes at pathology (11.8% vs. 5.8%, $P < 0.001$). Similarly, the pN1 rate (28.2% vs. 18.9%, $P < 0.001$), the number of removed LNs (median, 17 vs. 11; $P < 0.001$), and the rate of patients with more than 2 positive nodes (9.7 vs. 5.8, $P < 0.001$) were remarkably higher in patients from the hybrid-SNB than in patients from the non-SNB group. Compared with the ICG-SNB group, patients in the hybrid-SNB group had a lower pN1 rate (28% vs. 36%, $P < 0.001$) and a lower number of lymph nodes removed (median, 17 vs. 20; $P < 0.001$).

In multivariable models predicting pN1, being in the hybrid-SNB group (odds ratio [OR], 1.61; 95%CI, 1.18–2.20; $P = 0.002$) was an independent predictor of LNI detection at final pathology, compared with being in the non-SNB group, after accounting for all preoperative covariates including number of removed nodes. On the other hand, being in the ICG-SNB group did not reach independent predictor status when compared with being in the non-SNB group (OR, 1.35; 95%CI, 0.89–2.03; $P = 0.1$; Table 2)[ID]TBL2[/ID]. Compared with being in the ICG-SNB group, being in the hybrid-SNB group (OR, 1.19; 95%CI, 0.76–1.86;

$P = 0.4$) was not associated with a significant increase in LNI detection at final pathology.

Subsequently, we graphically represented the variation in pN1 detection rate for the hybrid-SNB technique versus the non-SNB technique across different preoperative LNI risk levels calculated according to the nomogram of Briganti et al. (Fig. 2) (*11*). Use of the hybrid-SNB approach was associated with a higher pN1 detection rate across all predicted levels of preoperative LNI risk.

Postoperative Complications

Overall, 572 (34%) patients experienced postoperative complications (Table 3). According to the Clavien–Dindo classification, 78 patients (4.6%) experienced grade I complications; 237 (14.1%), grade II; 128 (7.6%), grade IIIa; 72 (4.3%), grade IIIB; and 3 (0.2%), grade IV. The overall rate of complications that were at least grade II was 25.1%, 25.5%, and 30.2% in the non-SNB, ICG-SNB, and hybrid-SNB groups, respectively. Similarly, complications of at least grade IIIa were found in 11.8%, 11.2%, and 13.4% of patients in the respective groups.

In multivariable models, the ICG-SNB group was not associated with a higher rate of experiencing at least a grade II complication (OR 1.22, 95%CI 0.80–1.85, $P = 0.3$; Table 4) or at least a grade IIIa complication (OR, 1.02; 95%CI, 0.56–1.77; $P = 0.9$; Table 4), whereas the hybrid-SNB group tended to have a higher risk of at least a grade II complication (OR, 1.30; 95%CI, 0.98–1.70; $P = 0.059$; Table 4) but not of at least a grade III complication (OR, 1.16; 95%CI, 0.79–1.67; $P = 0.4$; Table 4). Of note, the year of surgery was associated with a reduced risk of complications that were at least grade II (OR, 0.927; 95%CI, 0.889–0.967; $P < 0.001$) or at least grade IIIa (OR, 0.922; 95%CI, 0.872–0.974; $P = 0.004$), demonstrating a reduction of complication rates over time (Table 4). Particularly, the interaction test for the hypothesis that refinements in SNB technique in more recent years reduced postoperative complication of grade II or higher was statistically significant for the hybrid-SNB group (OR, 0.90; 95%CI, 0.81–0.99; $P = 0.041$). Specifically, the risk of experiencing at least a grade II complication decreased approximately 10% every year when compared with the risk of experiencing at least a grade II complication with standard lymph node dissection. On the other hand, no significant interaction with year of surgery was recorded for the ICG-SNB group (Table 4).

Finally, no statistically significant interaction was found between the year of surgery and complications that were grade IIIa or higher; therefore, technical refinement of the SNB procedure over time did not affect the rate of severe complications (all $P > 0.05$).

Oncologic Outcomes

At 5 y of follow-up, unadjusted Kaplan–Meier plots depicted BCR-free survival rates of 54.9% for the non-SNB group, 38.4% for the ICG-SNB group, and 57.7% for the hybrid-SNB group ($P = 0.39$; Supplemental Fig. 1A; supplemental materials are available at http://jnm.snmjournals.org). Similarly, 5-y CR-free survival rates were 67%, 73%, and 67.4% ($P = 0.9$) for the respective groups (Supplemental Fig. 1B). In multivariable Cox models, being in the ICG-SNB group was not an independent predictor of BCR (hazard ratio [HR], 0.84; 95%CI, 0.61–1.15; $P = 0.2$) or CR (HR, 0.73; 95%CI, 0.49–1.15; $P = 0.1$), compared with being in the non-SNB group. Conversely, being in the hybrid-SNB

TABLE 2
Multivariable Logistic Regression Model Predicting Detection of Positive Nodes at Final Pathology

Variable	Parameter	OR	95%CI	P
cT stage	cT1c	Ref		
	cT2	1.14	0.74–1.79	0.4
	≥cT3	3.25	2.11–5.14	<0.001
Biopsy GS	6	Ref		
	7	1.99	1.20–3.46	0.009
	8–10	3.00	1.79–5.27	<0.001
cN stage	cNx	Ref		
	cN0	0.85	0.58–1.23	0.4
	cN1	3.02	1.84–4.98	<0.001
Percentage of positive cores		1.633	1.371–1.94	<0.001
PSA at RP		1.010	1.002–1.018	0.01
Number of removed nodes		1.032	1.015–1.049	<0.001
SNB use	Non-SNB	Ref		
	ICG SNB	1.35	0.89–2.03	0.1
	Hybrid SNB	1.61	1.18–2.20	0.002

Ref = reference; GS = Gleason score; PSA = prostate-specific antigen; RP = radical prostatectomy.

group was associated with a lower risk of BCR (HR, 0.79; 95%CI, 0.63–0.98; $P = 0.037$) and of CR (HR, 0.76; 95%CI, 0.58–0.98; $P = 0.035$) than was being in the non-SNB group (Table 5). As further confirmation of these results, when the hybrid-SNB group was considered a reference, the ICG-SNB group did not differ from it in BCR (HR, 1.06; 95%CI, 0.75–1.50; $P = 0.7$) or CR (HR, 0.97; 95%CI, 0.63–1.49; $P = 0.9$), whereas the non-SNB group had a higher risk of BCR (HR, 1.26; 95%CI, 1.01–1.57; $P = 0.037$) and CR (HR, 1.32; 95%CI, 1.02–1.71; $P = 0.035$). Graphical representations of the multivariable adjusted Cox-derived BCR- and CR-free survival using Kaplan–Meier plots are shown in Figures 3A and 3B.

DISCUSSION

In this largest (to our knowledge) retrospective series of prostate cancer patients treated with robot-assisted radical prostatectomy and ePLND with or without SNB, we tested the impact of SNB on different outcomes, namely LNI staging accuracy, complication rates, and midterm oncologic outcomes. These aims were based on recent literature suggesting a potential benefit from using SNB to detect nodal metastases outside the standard ePLND template (20). Additionally, other evidence suggested that the addition of SNB, compared with standard ePLND, is associated with a potential decrease in the BCR rate (5). Our analyses highlighted several important findings.

First, the findings in the non-SNB group underlined that meticulous ePLND does not ensure complete accuracy with regard to nodal status. Adding SNB to standard ePLND improved the LNI detection rate in univariable analysis.

Specifically, ICG–99mTc-nanocolloid allowed detection of 10% more LNI than did ePLND without SNB. Similarly, ICG was associated with an 18% absolute increase in the LNI detection rate, relative to standard ePLND (Table 1). Our results reinforce recent findings in a systematic review of the diagnostic accuracy of the SNB procedure in prostate cancer (4). In that review, the SN or SNs were the only metastatic site or sites in 73% of LN-positive patients, and positive LNs would have been missed without SNB in 1 of 20 patients who underwent ePLND (4). Our findings confirm that SNB should always be combined with ePLND, as supported by a recent SN consensus panel (21). Despite being in line with previous series based on tertiary-care referral centers (6, 22) or population-based data repositories (23), it may be argued that the lower lymph nodal yield in the non-SNB group (median, 11 nodes) than in the hybrid-SNB or ICG-SNB group might have affected the reported differences in LNI. However, we demonstrated for the first time (to our knowledge) that in a multivariable model accounting for multiple confounders including the number of nodes removed, there was diagnostic added value for the hybrid-SNB group (OR, 1.65) but not for the ICG-SNB group (OR, 1.35). This finding suggests that ICG extends the ePLND template without providing specific guidance on aberrant lymphatic drainage pathways, whereas the hybrid tracer highlights aberrant drainage profiles, impacting the ePLND template. The fact that these aberrant profiles are seen at preoperative imaging impacts the ePLND template used during surgery. Additionally, when we graphically explored the variation in the actual LNI rate for the hybrid-SNB group versus the non-SNB group across different levels of preoperative LNI risk, we
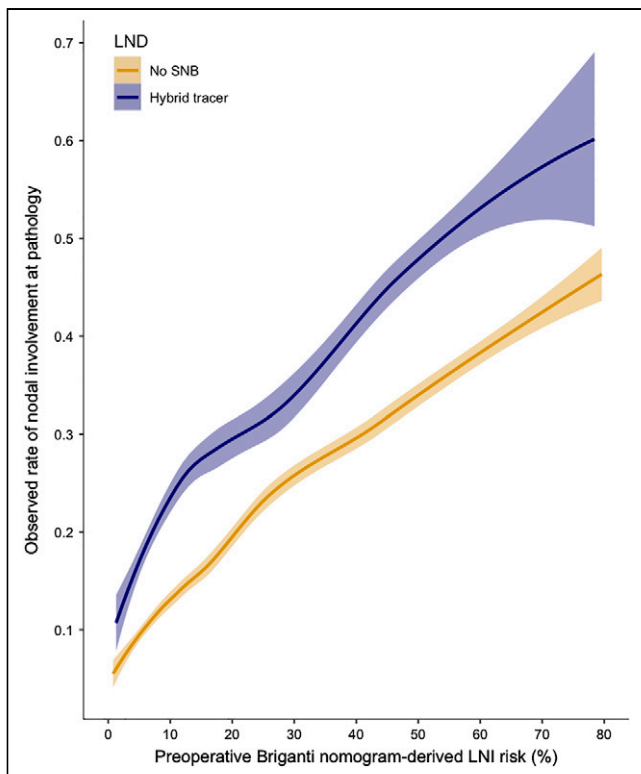
FIGURE 2. Locally weighted scatterplot smoothing plot representing observed LNI rate at final pathology plotted against preoperative predicted risk of nodal involvement calculated according to nomogram of Briganti et al. (11), stratified according to use of hybrid SNB or no SNB. LND = lymph node dissection.

confirmed that the hybrid-SNB approach was associated with a higher pN1 detection rate across all predicted levels of preoperative LNI risk, corroborating the accuracy of SNB in detecting pN1 both in low-risk and in high-risk patients. For instance, for a preoperative predicted risk of LNI of 20%, the

intraoperative guidance of the hybrid tracer can reduce the risk of false-negative findings by approximately 10%, meaning that in 1 of 10 patients who underwent lymph node dissection, a lymph nodal invasion would have been missed without using SNB with the hybrid tracer.

Second, when we assessed the safety profile of the SNB procedure, we observed that neither ICG SNB nor hybrid SNB was associated with an increased risk of postoperative complications that were at least Clavien–Dindo grade II. Thus, SNB appears to be safe and can be implemented in routine clinical practice without exposing patients to a higher risk of complications. Also, the interaction term between year of surgery and SNB showed a significant reduction of these grade II or higher complications over time for the hybrid tracer, which historically was also the first to be applied (non-SNB, 2006–2019; ICG SNB, 2016–2019; hybrid SNB, 2010–2019). This finding suggests that the time during which the hybrid tracer was used allowed for refinement of the surgical skill with which the SNB procedure was performed. This learning curve seems to have benefited the ICG-SNB group, which was the last to be initiated. Regarding high-grade complications (Clavien–Dindo grade ≥ III), we failed to observe any effect of year of surgery on SNB, suggesting that severe complications are not related to the SNB procedure. Lastly, the addition of SNB with a hybrid tracer was associated with a longer operative time than was needed for ePLND alone or for SNB with free ICG, probably because of the time needed to introduce and guide the laparoscopic γ-probe toward the target tissue. However, such differences were small (median, +6 min and +10 min, respectively; Table 1) and, in consequence, had a very limited clinical impact.

Third, when we explored the effect of SNB on oncologic outcomes, we found that the risk of BCR was significantly lower for the hybrid-SNB group than for the non-SNB group; there was a 20% lower risk of harboring BCR. We failed to observe this benefit for the ICG-SNB group. Our findings corroborated previous evidence that adding SNB to ePLND improves BCR-free survival (5), when we added a subanalysis according to type of SNB tracer used. This protective effect of

TABLE 3
Complication Rates and Grading

Variable	Parameter	Overall	Non-SNB, n = 1,168 (69.5%)	ICG SNB, n = 161 (9.6%)	Hybrid SNB, n = 351 (20.9%)
Any postoperative complication	No	1,108 (66)	777 (66.5)	115 (71.4)	216 (61.5)
	Yes	572 (34)	391 (33.5)	46 (28.6)	135 (38.5)
Clavien–Dindo grade*	I	78 (4.6)	58 (5)	4 (2.5)	16 (4.6)
	II	237 (14.1)	155 (13.3)	23 (14.3)	59 (16.8)
	IIIa	128 (7.6)	80 (6.8)	16 (9.9)	32 (9.1)
	IIIb	72 (4.3)	56 (4.8)	2 (1.2)	14 (4)
	IV	3 (0.2)	2 (0.2)	0 (0)	1 (0.3)
	Unknown	54 (3.2)	40 (3.4)	1 (0.6)	13 (3.7)

*Patients may have experienced more than one complication.
Data are number followed by percentage in parentheses.

Variable	Parameter	Grade ≥ 2				Grade ≥ 3			
		OR	2.5%	97.5%	P	OR	2.5%	97.5%	P
Age		1.008	0.990	1.027	0.3	1.025	1.000	1.052	0.046
Year of surgery		0.927	0.889	0.967	<0.001	0.922	0.872	0.974	0.004
SNB type	No SNB								
	ICG only	1.22	0.80	1.85	0.3	1.02	0.56	1.77	0.9
	ICG + ^{99m}Tc	1.30	0.98	1.70	0.059	1.16	0.79	1.67	0.4
cT stage	cT1c								
	cT2	0.87	0.64	1.20	0.4	1.01	0.66	1.56	0.9
	≥cT3	0.71	0.50	1.02	0.06	0.63	0.39	1.05	0.07
Biopsy GS	≤6								
	7	1.39	0.96	2.06	0.08	1.95	1.14	3.50	0.01
	8–10	1.62	1.09	2.44	0.01	1.66	0.94	3.07	0.08
cN stage	cN0								
	cNx	0.65	0.47	0.89	0.009	0.50	0.32	0.78	0.002
	cN1	0.90	0.52	1.49	0.7	1.35	0.68	2.46	0.3
PSA at surgery		0.989	0.978	0.998	0.038	0.998	0.986	1.008	0.8
Neo-ADT	No								
	Yes	1.14	0.79	1.62	0.4	1.34	0.84	2.09	0.1
SNB–year interaction	No SNB	Ref							
	SNB and ICG	1.41	0.97	2.12	0.08	1.21	0.75	2.11	0.4
	SNB and ICG + ^{99m}Tc	0.90	0.81	0.99	0.041	1.06	0.93	1.21	0.3

GS = Gleason score; PSA = prostate-specific antigen; ADT = androgen deprivation therapy; Ref = reference.

the hybrid tracer on BCR may be explained by the identification of aberrant lymphatic drainage pathways that are not usually included in standard lymph-node-dissection templates, thus optimizing nodal staging and improving patient management. Moreover, after adjusting for use of salvage radiation therapy, we confirmed the added value of the hybrid tracer when CR was assessed. Specifically, the hybrid tracer was associated with a significant, 24%, reduction in the risk of experiencing CR. These findings are noteworthy, and to the best of our knowledge, we are the first to demonstrate that adding SNB with a hybrid tracer to ePLND potentially reduces the risk of locoregional or distant recurrence. However, considering the relatively short follow-up and the limited number of events in our cohort, further studies are needed to confirm our results.

Recently, a new γ-probe for image-guided robotic surgery was developed (i.e., a drop-in probe) and implanted into clinical practice (24–27). Its increased maneuverability yielded a higher in vivo SN detection rate than that of a laparoscopic rigid γ-probe (25), suggesting that the impact of hybrid SNB might be further improved in future studies that rely on the drop-in probe as radioguidance in the robotic setting. It is also interesting that the FireFly fluorescence guidance realized within the hybrid-SNB group was achieved while injecting a 20-times-lower amount of ICG than in the ICG-SNB group.

Lastly, even though we did not specifically assess the cost of the SNB procedures in the current analysis, the SNB correlated with additional technologic resources (e.g., γ-probe, drop-in probes, and SPECT/CT), extra scanning time (fees vary across the health-care systems of different countries), and longer operative time, in turn increasing the overall costs of the procedure. Therefore, this point should be considered when SNB is implemented in a routine surgical practice. However, the prices of γ-probes are expected to decrease soon because of their expanding use and novel (hybrid) camera systems (28).

Despite its strengths, our study was not devoid of limitations. First, our report is based on a retrospective analysis, with all of its inherent limitations, and bias in selecting patients for specific methods of ePLND cannot be excluded. Second, our data reflect a single tertiary-care referral center with a high volume of SN procedures and trained surgeons for radioguided SN procedures. On the basis of the impact that nuclear medicine imaging had on the success of the hybrid-SNB group, the generalizability of our findings may be limited to centers with a nuclear medicine department. Third, the median follow-up was relatively short. Future randomized controlled trials are needed to confirm the findings reported here. Fourth, the fact that the ICG-SNB group was considerably smaller than the hybrid-SNB group might have influenced

TABLE 5
Multivariable Cox Regression Models Predicting BCR and CR in Patients Undergoing ePLND With or Without SNB

Variable	Parameter	BCR			BCR		
		HR	95%CI	P	HR	95%CI	P
SNB technique	Non-SNB	Ref					
	ICG SNB	0.84	0.61–1.15	0.2	0.73	0.49–1.11	0.1
	Hybrid SNB	0.79	0.63–0.98	0.037	0.76	0.58–0.98	0.035
pN stage	pN0						
	pN1	3.11	2.59–3.72	<0.001	3.40	2.74–4.23	<0.001
PSA at surgery		1.009	1.006–1.01	<0.001	1.010	1.006–1.014	<0.001
Pathologic GS	6						
	7	1.91	1.17–3.10	0.009	3.77	1.53–9.26	0.003
	8–10	3.50	2.13–5.74	<0.001	8.84	3.59–21.7	<0.001
pT stage	≤pT2c						
	pT3a	1.63	1.30–2.06	<0.001	1.99	1.50–2.64	<0.001
	≥pT3b	2.17	1.74–2.71	<0.001	2.17	1.66–2.85	<0.001
PSM	No						
	Yes	1.23	1.04–1.46	0.01	0.93	0.76–1.14	0.5
Number of removed nodes		1.005	0.994–1.018	0.3	1.00	0.985–1.015	0.9
Salvage radiation therapy	No	–			Ref		
	Yes	–			1.29	0.92–1.58	0.1

Ref = reference; PSA = prostate-specific antigen; GS = Gleason score; PSM = positive surgical margins.
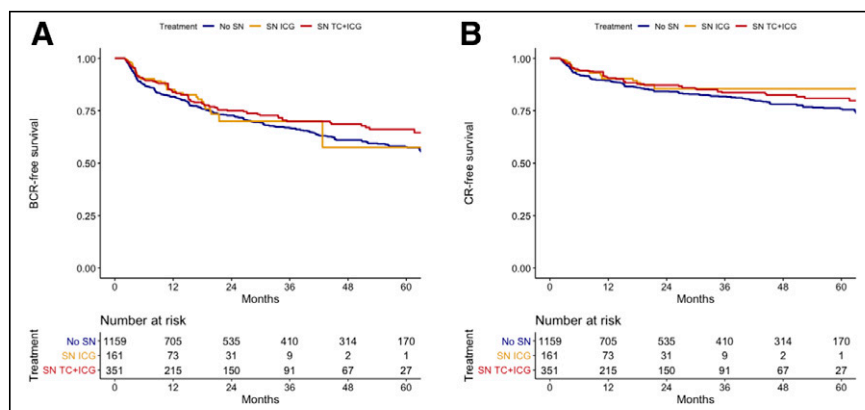

FIGURE 3. Kaplan–Meier plots depicting multivariable Cox-derived BCR-free (A) and CR-free (B) survival after robot-assisted radical prostatectomy and ePLND with or without use of additional SNB (either hybrid tracer or free ICG). TC = ^{99m}Tc.

our findings; this possibility needs further validation in a bigger sample size. Lastly, the current study did not involve the use of hybrid tracers relying on prostate cancer–specific biomarkers such as ^{99m}Tc-based prostate-specific membrane antigen (^{99m}Tc-PSMA). However, despite having a lower specificity for prostatic tissue than ^{99m}Tc-PSMA does, the ICG–^{99m}Tc-nanocolloid tracer has important advantages. It allows intraoperative delineation of the lymphatic drainage profile of the prostate—

something not possible with PSMA-based tracers, which, conversely, allow identification of metastatic lesions, when present, but not definition of the lymphatic drainage profile. Moreover, the intraoperative use of PSMA-based tracers was tested mainly in the context of recurrent prostate cancer in patients with a positive lesion on preoperative PET/CT (29); therefore, its utility and staging accuracy in the primary treatment of intermediate- or high-risk patients is still under evaluation.

CONCLUSION

SNB with the hybrid tracer ICG–^{99m}Tc-nanocolloid improves the LNI detection rate in prostate cancer patients, reducing the risk of false-negative findings at final pathology without increasing postoperative complications. Moreover, we find that this method may have a potential benefit in terms of BCR and CR.

DISCLOSURE

KEY POINTS

QUESTION: Is the implementation of SNB for prostate cancer able to improve nodal staging and, consequently, oncologic outcomes in patients receiving radical prostatectomy and lymph node dissection?

PERTINENT FINDINGS: The use of ICG–^{99m}Tc-nanocolloid tracer was an independent predictor of nodal involvement and lower BCR and CR rates, whereas the use of free ICG did not reach independent predictor status, when compared with the use of no SNB.

IMPLICATIONS FOR PATIENT CARE: The implementation of hybrid-SNB technique in prostate cancer improves detection of positive nodes and allows subsequent optimization of patient management without harming patient safety.

REFERENCES

1. Fossati N, Willemse PPM, Van den Broeck T, et al. The benefits and harms of different extents of lymph node dissection during radical prostatectomy for prostate cancer: a systematic review. *Eur Urol.* 2017;72:84–109.

2. Mottet N, van den Bergh RCN, Briers E, et al. EAU-EANM-ESTRO-ESUR-SIOG guidelines on prostate cancer—2020 update. Part 1: screening, diagnosis, and local treatment with curative intent. *Eur Urol.* 2021;79:243–262.

3. Harke NN, Godes M, Wagner C, et al. Fluorescence-supported lymphography and extended pelvic lymph node dissection in robot-assisted radical prostatectomy: a prospective, randomized trial. *World J Urol.* 2018;36:1817–1823.

4. Wit EMK, Acar C, Grivas N, et al. Sentinel node procedure in prostate cancer: a systematic review to assess diagnostic accuracy. *Eur Urol.* 2017;71:596–605.

5. Grivas N, Wit EMK, Kuusk T, et al. The impact of adding sentinel node biopsy to extended pelvic lymph node dissection on biochemical recurrence in prostate cancer patients treated with robot-assisted radical prostatectomy. *J Nucl Med.* 2018;59:204–209.

6. Mazzone E, Preisser F, Nazzani S, et al. The effect of lymph node dissection in metastatic prostate cancer patients treated with radical prostatectomy: a contemporary analysis of survival and early postoperative outcomes. *Eur Urol Oncol.* 2019;2:541–548.

7. Ventimiglia E, Seisen T, Abdollah F, et al. A systematic review of the role of definitive local treatment in patients with clinically lymph node-positive prostate cancer. *Eur Urol Oncol.* 2019;2:294–301.

8. van Leeuwen AC, Buckle T, Bendle G, et al. Tracer-cocktail injections for combined pre- and intraoperative multimodal imaging of lymph nodes in a spontaneous mouse prostate tumor model. *J Biomed Opt.* 2011;16:016004.

9. Schaafsma BE, Verbeek FPR, Rietbergen DDD, et al. Clinical trial of combined radio- and fluorescence-guided sentinel lymph node biopsy in breast cancer. *Br J Surg.* 2013;100:1037–1044.

10. Cacciamani GE, Shakir A, Tafuri A, et al. Best practices in near-infrared fluorescence imaging with indocyanine green (NIRF/ICG)-guided robotic urologic surgery: a systematic review-based expert consensus. *World J Urol.* 2020;38:883–896.

11. Briganti A, Larcher A, Abdollah F, et al. Updated nomogram predicting lymph node invasion in patients with prostate cancer undergoing extended pelvic lymph node dissection: the essential importance of percentage of positive cores. *Eur Urol.* 2012;61:480–487.

12. Hueting TA, Cornel EB, Somford DM, et al. External validation of models predicting the probability of lymph node involvement in prostate cancer patients. *Eur Urol Oncol.* 2018;1:411–417.

13. KleinJan GH, van den Berg NS, Brouwer OR, et al. Optimisation of fluorescence guidance during robot-assisted laparoscopic sentinel node biopsy for prostate cancer. *Eur Urol.* 2014;66:991–998.

14. van der Poel HG, Buckle T, Brouwer OR, Valdés Olmos RA, van Leeuwen FWB. Intraoperative laparoscopic fluorescence guidance to the sentinel lymph node in prostate cancer patients: clinical proof of concept of an integrated functional imaging approach using a multimodal tracer. *Eur Urol.* 2011;60:826–833.

15. KleinJan GH, van den Berg NS, de Jong J, et al. Multimodal hybrid imaging agents for sentinel node mapping as a means to (re)connect nuclear medicine to advances made in robot-assisted surgery. *Eur J Nucl Med Mol Imaging.* 2016;43:1278–1287.

16. Dindo D, Demartines N, Clavien PA. Classification of surgical complications: a new proposal with evaluation in a cohort of 6336 patients and results of a survey. *Ann Surg.* 2004;240:205–213.

17. Assel M, Sjoberg D, Elders A, et al. Guidelines for reporting of statistics for clinical research in urology. *Eur Urol.* 2019;75:358–367.

18. Dell'Oglio P, Mazzone E, Lambert E, et al. The effect of surgical experience on perioperative and oncological outcomes after robot-assisted radical cystectomy with intracorporeal urinary diversion: evidence from a high-volume center. *Eur Urol Suppl.* 2019;18:e2637–e2639.

19. Cleveland WS. Robust locally weighted regression and smoothing scatterplots. *J Am Stat Assoc.* 1979;74:829–836.

20. Preisser F, Bandini M, Marchioni M, et al. Extent of lymph node dissection improves survival in prostate cancer patients treated with radical prostatectomy without lymph node invasion. *Prostate.* 2018;78:469–475.

21. van der Poel HG, Wit EM, Acar C, et al. Sentinel node biopsy for prostate cancer: report from a consensus panel meeting. *BJU Int.* 2017;120:204–211.

22. Poelaert F, Joniau S, Roumeguère T, et al. Current management of pT3b prostate cancer after robot-assisted laparoscopic prostatectomy. *Eur Urol Oncol.* 2019;2:110–117.

23. Mazzone E, Dell'Oglio P, Rosiello G, et al. Technical refinements in superextended robot-assisted radical prostatectomy for locally advanced prostate cancer patients at multiparametric magnetic resonance imaging. *Eur Urol.* September 14, 2020 [Epub ahead of print].

24. Collamati F, van Oosterom MN, De Simoni M, et al. A DROP-IN beta probe for robot-assisted ^{68}Ga-PSMA radioguided surgery: first ex vivo technology evaluation using prostate cancer specimens. *EJNMMI Res.* 2020;10:92.

25. Dell'Oglio P, Meershoek P, Maurer T, et al. A DROP-IN gamma probe for robot-assisted radioguided surgery of lymph nodes during radical prostatectomy. *Eur Urol.* 2021;79:124–132.

26. Meershoek P, van Oosterom MN, Simon H, et al. Robot-assisted laparoscopic surgery using DROP-IN radioguidance: first-in-human translation. *Eur J Nucl Med Mol Imaging.* 2019;46:49–53.

27. van Oosterom MN, Simon H, et al. Revolutionizing (robot-assisted) laparoscopic gamma tracing using a drop-in gamma probe technology. *Am J Nucl Med Mol Imaging.* 2016;6:1–17.

28. Dell'Oglio P, de Vries HM, Mazzone E, et al. Hybrid indocyanine green–^{99m}Tc-nanocolloid for single-photon emission computed tomography and combined radio- and fluorescence-guided sentinel node biopsy in penile cancer: results of 740 inguinal basins assessed at a single institution. *Eur Urol.* 2020;78:865–872.

29. Maurer T, Robu S, Schottelius M, et al. ^{99m}Technetium-based prostate-specific membrane antigen-radioguided surgery in recurrent prostate cancer. *Eur Urol.* 2019;75:659–666.